Molecular Crystals and Liquid Crystals
Publication details, including instructions for authors and subscription information:
http://www.tandfonline.com/loi/gmcl16

Dynamics of the Freedericksz Transition in the Electric Field in Non Ideally Oriented Nematic Layers at Subthreshold and Above Threshold Voltages

N. Aneva [a], A. G. Petrov [b], S. Sokerov [c] & S. P. Stoylov [c]

[a] Department of Physical Chemistry, University of Sofia, Bulgaria

[b] Institute of Solid State Physics, Bulgarian Academy of Sciences, 1113, Sofia, Bulgaria

[c] Institute of Physical Chemistry, Bulgarian Academy of Sciences, 1040, Sofia, Bulgaria

Version of record first published: 20 Apr 2011.

To cite this article: N. Aneva , A. G. Petrov , S. Sokerov & S. P. Stoylov (1980): Dynamics of the Freedericksz Transition in the Electric Field in Non Ideally Oriented Nematic Layers at Subthreshold and Above Threshold Voltages, Molecular Crystals and Liquid Crystals, 60:1-2, 1-19

To link to this article: http://dx.doi.org/10.1080/00268948008072421

Mol. Cryst. Liq. Cryst., 1980, Vol. 60, pp. 1–20
0026-8941/80/6001–0001$04.50/0

Printed in the U.S.A.

Dynamics of the Freedericksz Transition in the Electric Field in Non Ideally Oriented Nematic Layers at Subthreshold and Above Threshold Voltages

N. ANEVA

Department of Physical Chemistry, University of Sofia, Bulgaria

and

A. G. PETROV

Institute of Solid State Physics, Bulgarian Academy of Sciences, 1113 Sofia, Bulgaria

and

S. SOKEROV and S. P. STOYLOV

Institute of Physical Chemistry, Bulgarian Academy of Sciences, 1040 Sofia, Bulgaria

(*Received June 18, 1979; in final form October 3, 1979*)

1 INTRODUCTION

The DAP†-effect was observed for the first time[1] in 1971 and in the last years has been largely investigated experimentally and theoretically.[2–8] In all the studies the close analogy of the DAP-effect to the Freedericksz[9] transition in magnetic field is emphasized. At that particular attention was paid to the threshold character of the DAP-effect, studying its static and dynamic characteristics and the effect of different factors on them. Recently

† DAP–Deformation of Aligned Phases.

statics and dynamics of the Freederickz transition were studied in details.[10–12]

The theoretical interpretation of these studies rest in a large part on two essential assumptions (in some works only one of them is made):

A) It is accepted that the orientation of the director **n** in close proximity to the electrode does not change. In this case which we shall call a case of "hard" boundary conditions, the theory predicts no dependence of the threshold voltage V_{th} on the liquid crystal layer thickness d

$$V_{th} = \pi\sqrt{\frac{K_{33}}{\Delta\chi}}$$

B) It is accepted, that initially the director **n** is oriented exactly parallel to the electric field **E**, so that $\mathbf{n} \times \mathbf{E} = 0$ for the whole liquid crystal layer. In this case of "ideal initial orientation" the theory predicts no layer deformation at subthreshold voltages $V < V_{th}$ and the effects begin with a sharp threshold at V_{th}.

However these assumptions are practically never satisfied and as Rapini and Papoular[13] have shown for the first time, when (A) is not satisfied, i.e. at "soft" boundary conditions the effect keeps its threshold character but V_{th} falls with the decrease of the layer thickness d. This is manifested particularly sharply when d is of the order of the "extrapolation length" $b = K_{33}/C$ (K_{33}—elastic constant, C—anchoring energy.)[15] The anchoring energy C characterizes the orientational interaction between the liquid crystal and the electrode and may vary in a wide range from 1 erg/cm^2 corresponding to "almost hard" boundary conditions ($b = 10^{-2}$ μm) to 10^{-4} erg/cm^2 ($b = 100$ μm), depending on the electrode treatment and the orientation of the director with respect to them. The influence of the "soft" boundary conditions on the statics and the dynamics of the effect was theoretically investigated by Nehring *et al.*[19]

In[13] it was also shown, that when the assumption (B) is not satisfied, the effect loses its threshold character. The layer deformation (although too weak) is already obtained even at subthreshold voltages, at threshold voltage only sharp increase in the deformation is observed. It seems that in this case it is more correct to speak for "subthreshold" and "above threshold" regimes of deformation and for "limiting voltage" V_c separating the two regimes. Independently from us this question was studied by other researchers.[20–22]

In this work we study the DAP-effect in homeotropic layers of ZLI-207 —commercial room temperature liquid crystal of MERCK—a negative dielectric anisotropy mixture ($\Delta\varepsilon = -0.6$) of azoxycompounds and aromatic esters with additives for spontaneous homeotropic orientation. The homeo-

tropic orientation was nonideal which was obtained by rubbing of the electrodes. The rubbing was made with the aim a plane of preferred deformation to be defined and in this manner to avoid the creation of umblics.[18] The nonideal initial orientation resulted in subthreshold deformations, the dynamics of which is further systematically studied experimentally and theoretically. This investigation was started in 1974 (see Ref. 23). The results described here have been reported in 1976 (see Ref. 24).

2 THEORY

Usually the theoretical description of the DAP-effect is made on the basis of the equation of the torque balance:

$$K_{33}\frac{\partial^2\theta}{\partial z^2} + \Delta\chi E^2 \sin\theta\cos\theta = \gamma_1\frac{\partial\theta}{\partial t}, \tag{1}$$

where K_{33} is the bend elastic constant, $\Delta\chi = |\Delta\varepsilon|/4\pi$ is the absolute value of the permittivity anisotropy, γ_1—the rotational viscosity of the liquid crystal and θ is the angle between the director $\mathbf{n}$ and the direction of the electric field $\mathbf{E}$, which is chosen to coincide with the OZ-axis of the introduced coordinate system.

In the one dimensional case with assumptions (A) and (B) both fulfilled $\theta(z, t)$ will satisfy the following boundary conditions:

$$\begin{aligned} \theta(z, 0) &= 0 \qquad \text{for } t = 0 \\ \theta\left(\frac{d}{2}, t\right) &= 0 \qquad \text{for } z = \pm\frac{d}{2} \end{aligned} \tag{2}$$

In our theoretical considerations which are restricted to the region of subthreshold and slightly above the threshold voltages we are not going to consider in details the role of the back-flow;[12,14] however we shall always have in mind that the rotational viscosity γ_1 in (1) is in reality the corrected for the back-flow effect quantity γ_1^*:

$$\frac{V}{V_c} \gtrsim 1 : \gamma_1^*\left(\frac{V}{V_c}\right) = \left(1 - \frac{A}{6}\right)\gamma_1; \tag{3}$$

for MBBA $\gamma_1^* = 0.875\,\gamma_1$, $A = f(\alpha_i)$ is a function of the Leslie's coefficients.[11]

The linearized equation, describing the steady-state deformation could be derived from (1) by suggesting that $\gamma_1\,\partial\theta/\partial t = 0$:

$$\xi^2\frac{\partial^2\theta}{\partial z^2} + \theta = 0, \frac{1}{\xi^2} = \frac{\Delta\chi E^2}{K_{33}}, \tag{4}$$

at boundary conditions

$$\theta\left(\pm\frac{d}{2}\right) = 0. \tag{5}$$

A solution of (4) satisfying (5) is

$$\theta = \theta_M \cos\frac{\pi z}{d}. \tag{6}$$

The substitution of (6) in (4) shows that for all voltages by which $1/\xi < \pi/d$, the only value of θ_M, for which (4) is satisfied is $\theta \equiv 0$. Only when $1/\xi$ reaches π/d, i.e. V reaches the threshold voltage V_c

$$V_c = \pi\sqrt{\frac{K_{33}}{\Delta\chi}}, \tag{7}$$

the Eq. (4) gets a non-zero solution in the form (6). The linear approximation does not provide the possibility to determine the constant θ_M. Its determination is performed in[10] by including the non-linear term $\frac{2}{2}\theta^3$ in (4):

$$\theta_M^2 = 2\left[1 - \left(\frac{V_c}{V}\right)^2\right] \qquad \text{for } V > V_c. \tag{8}$$

As it has been already mentioned, our theoretical model leaves off the both assumptions (A) and (B), i.e. a non-ideally oriented layer with "soft" boundary conditions is considered. This represents a generalization of the results given in[13] leaving off each of the assumptions separately.

2.1 Steady-state

In the case of hard boundary conditions instead of (5) we have

$$\theta\left(\pm\frac{d}{2}\right) = \theta_0, \tag{9}$$

where θ_0 is a small angle, describing the initial deviation of the director from the normal to the electrode due to its treatment. For simplification it is accepted that this angle is the same at the two boundaries.

At finite values of the anchoring energy C (weak anchoring) the boundary conditions for the angle $\theta(\pm d/2)$ are substituted by the conditions for the balance of the elastic torques on the boundaries, since the orientation of the

director there can change. These conditions in linear approximation by ideal initial orientation can be represented as:[15]

$$\left.\frac{d\theta}{dz}\right|_{z=d/2} = -\frac{1}{b}\theta\Big|_{z=d/2}, \qquad \left.\frac{d\theta}{dz}\right|_{z=-d/2} = \frac{1}{b}\theta\Big|_{z=-d/2} \tag{10}$$

For solutions $\theta(z)$ which are even functions of z Eq. (10) is reduced to one condition at $z = d/2$ and to the condition

$$\left.\frac{d\theta}{dz}\right|_{z=0} = 0.$$

In order to take into account in the same time also the nonideal initial orientation (10) can be written in the form:

$$\left.\frac{d\theta}{dz}\right|_{z=d/2} = -\frac{1}{b}(\theta|_{z=d/2} - \theta_0), \qquad \left.\frac{d\theta}{dz}\right|_{z=0} = 0 \tag{11}$$

This condition means that the elastic torques, due to surface energy are minimal at $\theta|_{d/2} = \theta_0$. The condition (11) gives at $V = 0$ initial solution $\theta(z) = \theta_0 = \text{const}$.

For $V > 0$ the solution has the form: $\theta(z) = \theta_M \cos(z/\xi)$, where

$$\theta_M = \frac{\theta_0}{\cos\frac{d}{2\xi} - \frac{b}{\xi}\sin\frac{d}{2\xi}} = \frac{\theta_0}{\cos\left(\frac{\pi}{2}\frac{V}{V_c}\right) - \frac{b}{d}\left(\pi\frac{V}{V_c}\right)\sin\left(\frac{\pi}{2}\frac{V}{V_c}\right)} \tag{12}$$

In this case θ_M increases sharply, when $V \to V_c'$, where V_c' is a solution of the equation of Rapini[13] expressing the condition for the denominator of θ_M in (12) to become zero:

$$\operatorname{cotg}\left(\frac{\pi}{2}\frac{V_c'}{V_c}\right) = \frac{b}{d}\left(\pi\frac{V_c'}{V_c}\right) \tag{13}$$

For cases of layer thickness, much greater than the extrapolation length (13) has the approximative solution

$$\frac{V_c'}{V_c} = \frac{d}{d+2b}, \; d \gg b \tag{14}$$

which clearly shows that with the decrease in the thickness d the limiting voltage V_c' falls.

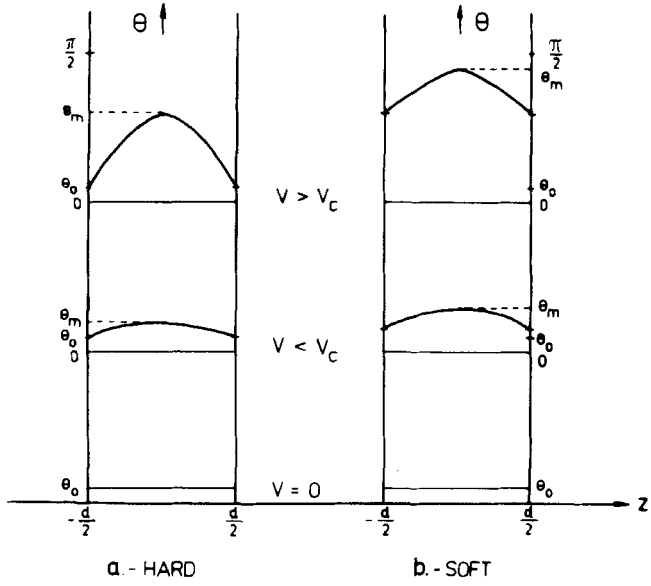

FIGURE 1 Schematic shape of the steady state distortion at hard (a) and soft (b) boundary conditions.

From (12) it is seen that the deformation is present for any voltage $V > 0$, but initially θ_M is very near to θ_0, i.e. the deformation is small. However, it strongly increases when V approaches V_c'. The fact that for $V \to V_c', \theta_M \to \infty$ is due to the linearization performed. In reality the increase of θ_M is limited by the non-linear terms. To calculate the voltage dependence of θ_M at $V > V_c'$ one has to solve the non-linear Eq. (1) with nonhomogeneous boundary conditions (11), which is not attempted here. In the case $\theta_0 = 0$ this dependence is given above—Eq. (8).

To get the solution at hard boundary conditions one has to put $b = 0$ in the Eq. (12). In this case $V_c' \equiv V_c$. The expected shapes of the layer distortions at different voltages are visualized in Figure 1a. Comparing to that, the situation at soft boundary conditions is depicted on Figure 1b. Due to the weak anchoring a variation of the boundary angle is observed as well, whereas in the case of Figure 1a it is fixed.

2.2 Dynamics

2.2.1 Hard boundary conditions, switching on the field We are looking for a solution of the linearized form of Eq. (1)

$$\xi^2 \frac{\partial^2 \theta}{\partial z^2} + \theta = \lambda \frac{\partial \theta}{\partial t}, \qquad \lambda = \frac{\gamma_1}{\Delta \chi E^2} \tag{15}$$

by initial and boundary conditions

$$\theta(z, 0) = \theta_0,$$
$$\theta\left(\pm \frac{d}{2}, t\right) = \theta_0. \tag{16}$$

The solution of this is got in the form

$$\theta(z, t) = \theta_\infty(z) + \theta'(z, t) \tag{17}$$

where $\theta_\infty(z)$ is the steady-state solution (9), and $\theta'(z, t)$ is

$$\theta'(z, t) = \sum_{n=1}^{\infty} A_n \exp\left[-\frac{t}{\lambda}\left[\left(\frac{n\pi\xi}{d}\right)^2 - 1\right]\right]\cos\frac{n\pi z}{d}$$
$$= -4\theta_0 \sum_{k=1}^{\infty} \frac{(-1)^{k+1}\cos\dfrac{(2k-1)\pi z}{d}}{(2k-1)\pi\left[\dfrac{(2k-1)^2\pi^2\xi^2}{d^2} - 1\right]}$$
$$\times \exp\left[-\frac{t}{\lambda}\left[\frac{(2k-1)^2\pi^2\xi^2}{d^2} - 1\right]\right]$$

This solution cannot be used for $V > V_c$. The divergence of the first coefficient ($k = 1$) at $V \to V_c$ simply reflects the divergence of the steady state solution. The reason is again the neglecting of non-linear terms (see the discussion after Eq. 14).

The even harmonics do not participate in the solution, since they do not satisfy the boundary conditions. Let us consider this solution in greater details. We see that the different harmonics are characterised by different relaxation times

$$\tau_n = \frac{\lambda}{\left(\dfrac{n\pi\xi}{d}\right)^2 - 1} = \frac{\lambda}{\left(\dfrac{nV_c}{V}\right)^2 - 1} = \frac{\dfrac{\gamma_1 d^2}{\Delta\chi}}{(nV_c)^2 - V^2}, \tag{18}$$

from which the longest is the first harmonic:

$$\tau_1 = \frac{\gamma_1}{\Delta\chi}\frac{d^2}{V_c^2 - V^2}.$$

This relaxation time essentially determines the relaxation behaviour of the system for times $t > \tau_3$. Therefore the dynamics of the system is well described by the law $1 - e^{-t/\tau_1}$. This makes the dynamics for subthreshold voltages to be qualitatively different from the dynamics for above threshold voltages.

The latter is characterized with a fast exponential growth in the beginning following the law e^{-t/τ_1} (at $V > V_c$, τ_1 given by (19) becomes negative), limited further by non-linear effects.[11] So one can write for comparison:

$$V < V_c,\ \theta_M(t) \sim \theta_0(1 - ae^{-t/\tau_1^-}),\ \tau_1^- = \frac{\gamma_1(d^2/\Delta\chi)}{V_c^2 - V^2},\ a < 1,\ t > \tau_3. \quad (20')$$

$$V > V_c,\ \theta_M(t) \sim \theta_0 e^{t/\tau_1^+},\ \tau_1^+ = \frac{\gamma_1(d^2/\Delta\chi)}{V^2 - V_c^2}. \quad (20'')$$

The Eq. (20″) is taken from the paper[11] (Eq. III.15a) where however θ_0 is due to the thermal fluctuations ($\langle\theta_0^2\rangle \sim kT$) and in the formula for the relaxation time (Eq. III.18) V_c^2/d^2 instead of H_c^2 is substituted.

It is seen from (20) that both times of relaxation tend to infinity in the vicinity of V_c. In fact near to the threshold ($V \gtrsim (\frac{2}{\pi})V_c$) the small angle approximation is no longer valid (see the discussion after Eq. 14). That's why a real divergence could not be expected. Rather, a sewing together of both expressions (20′) and (20″) in a maximum in the dependence $\tau_1(V)$ is to take place and our experimental data, presented here and in the previous paper of ours[25] really demonstrate the existence of such a maximum.

Switching off of the field The relaxation back to the initial state is described by the equation:

$$K_{33}\frac{\partial^2\theta}{\partial z^2} = \gamma_1\frac{\partial\theta}{\partial t}, \quad (21)$$

by initial and boundary conditions

$$\theta(z_1\ 0) = \theta_M \cos\frac{z}{\xi},$$
$$\theta\left(\pm\frac{d}{2}, t\right) = \theta_0. \quad (22)$$

The solution of this equation is obtained in the form:

$$\theta(z, t) = \theta_0 + \sum_{n=1}^{\infty} B_n e^{-t/\sigma_n}\cos\frac{n\pi z}{d},$$

where

$$\sigma_n = \frac{\gamma_1 d^2}{n^2\pi^2 K_{33}} \quad \text{and} \quad B_n = -A_n,$$

i.e.

$$\theta(z, t) = \theta_0 + 4\theta_0\sum_{k=1}^{\infty}\frac{(-1)^{k+1}\exp-(t/\sigma_{2k-1})}{(2k-1)\pi\left[\frac{(2k-1)^2\pi^2\xi^2}{d^2} - 1\right]}\cos\frac{(2k-1)\pi z}{d}. \quad (23)$$

The most slowly fading harmonic in this case is characterized with the time of fading

$$\sigma_1 = \frac{\gamma_1 d^2}{\pi^2 K_{33}}. \tag{24}$$

In this case the theory predicts, that the relaxation time has to rise with the square of layer thickness, which as we shall see further is not satisfied experimentally.

2.2.2 Soft boundary conditions. Switching on of the field The Eq. (15) by initial conditions

$$\theta(z, 0) = \theta_0$$

and boundary conditions (11) has the solution:

$$\theta(z, t) = \theta_M \cos\frac{z}{\xi} - 4\theta_0 \sum_{n=1}^{\infty} \frac{(-1)^{n+1}\,\dfrac{d}{b}\sqrt{\alpha_n^2 + \left(\dfrac{d}{b}\right)^2}\exp - \dfrac{t}{\lambda}\left[\left(\dfrac{\alpha_n \xi}{d}\right)^2 - 1\right]}{\alpha_n\left[\alpha_n^2 + \dfrac{2d}{b} + \left(\dfrac{d}{b}\right)^2\right]\left[\left(\dfrac{\alpha_n \xi}{d}\right)^2 - 1\right]} \cos\frac{\alpha_n z}{d} \tag{25}$$

where b is the extrapolation length, θ_M is given by (12) and α_n are the solutions of the transcendental equation

$$\operatorname{cotg}\frac{\alpha_n}{2} = \frac{b}{d}\alpha_n, \tag{26}$$

forming a monotonically growing series. Here again longest time of reaching the steady state has the first harmonic:

$$\tau = \frac{\lambda}{\left(\dfrac{\alpha_1 \xi}{d}\right)^2 - 1} \tag{27}$$

and the relaxation behaviour of the system is determined essentially by it. The expression for τ_1, shows that it tends to infinity by $d/\xi \to 1$. Taking into account that α_1 is the smallest root of the equation (26) when substituting with d/ξ we find that the critical value of ξ is given by the equation

cotg $d/2\xi = (b/d)(d/\xi)$, which coincides with the equation for the critical voltage V_c' (13), so that τ_1 can be written in the form:

$$\tau_1 = \frac{\gamma_1}{\Delta\chi}\frac{d^2}{V_c'^2 - V^2}\left(V_c' = \frac{\alpha_1}{\pi}V_c\right), \tag{28}$$

and again, as in the case of hard boundary conditions, it tends to infinity in the vicinity of the critical voltage V_c'.

Switching off of the field The solution of (21) in this case is:

$$\theta(z, t) = \theta_0 + 4\theta_0 \sum_{n=1}^{\infty} \frac{(-1)^{n+1}\dfrac{d}{b}\sqrt{\alpha_n^2 + \left(\dfrac{d}{b}\right)^2}\, e^{-t/\sigma_n}}{\alpha_n\left[\alpha_n^2 + \dfrac{2d}{b} + \left(\dfrac{2d}{b}\right)^2\right]\left[\left(\dfrac{\alpha_n\xi}{d}\right)^2 - 1\right]} \cos\frac{\alpha_n z}{d}, \tag{29}$$

where

$$\sigma_n = \frac{\gamma_1 d^2}{\alpha_n^2 K_{33}} \tag{30}$$

are the decay times of the different harmonics. The most slowly fading harmonic gas a relaxation time σ_1. In the case of $d/b \gg 1$, α is given by the approximate solution of (26).

$$\alpha_1 = \frac{\pi}{1 + 2b/d}, \tag{31}$$

i.e.

$$\sigma_1 = \frac{1}{\pi^2}\frac{\gamma_1}{K_{33}}(d + 2b)^2. \tag{32}$$

It is clear that by soft boundary conditions the relation $\sigma \sim d^2$ is not followed.

3 EXPERIMENT

The experimental set up is described in details in a previous work of ours,[25] where also a part of the results is presented. The liquid crystal cell is placed between crossed polaroids. The light which passes through the cell is further measured by a photomultiplier. The experimental set up is shown on Figure 2.

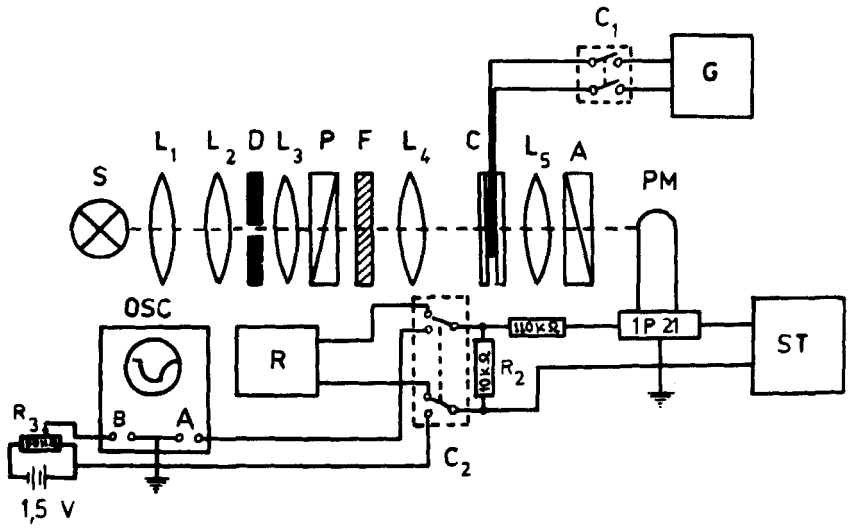

FIGURE 2 Experimental set-up. S—light source-incandescent lamp TUNGSRAM 8 V, 50 W; L_1–L_5—lenses; D-slit; F-filter-type SIF, λ-600–1000 nm; C-liquid crystal cell; P-polariser; A-analiser; C_1, C_2—switches; PM-photomultiplier-type RCA 1P 21; R-recording device Servegor-Georz 1PE; R_1, R_2, R_3-resistances; OSC-oscilloscope-ORION-EMG with differential amplifier; ST—high voltage stabilizer; G—generator-Cleamann-Grahnert for alternating voltage (10 Hz–1 MHz).

At crossed polaroids the intensity of the transmitted light I_x is connected with the angle of inclination $\theta(z)$ by the formula:

$$I_x = I_0 \sin^2 \frac{\delta}{2} = I_0 \sin^2 \left[\frac{\pi}{\lambda} \frac{n_0}{2} \left(1 - \frac{n_0^2}{n_e^2} \right) \int_{-d/2}^{d/2} \sin^2 \theta(z) dz \right], \qquad (33)$$

where I_0 is the intensity of the incident light, d is the thickness of the liquid crystal layer and n_e, n_0 are the refractive indexes of the liquid crystal. Equation (33) holds for the case when the plane of the initial inclination makes an angle of 45° with the plane of polarization.

From the experimentally measured initial transmittance (see below) and using the catalogue data of Merck[16] for the birefringence of the used material ZLI-207: $\Delta n = 0.29$ the following very rough value of

$$\theta_0 = 0.1 \text{ rad}$$

can be estimated for the initial inclination. This initial inclination as it was already considered above is responsible for the nonthreshold behaviour of the DAP-effect. This is illustrated on Figure 3 and Figure 6. On Figure 3 the contrast ratio of the effect $K = I(V)/I_0[\%]$ is plotted as a function of the voltage. On Figure 6 (right ordinate axis) the phase difference δ using maxima points in $K(V)$ dependence from Figure 3 is plotted as well. Both

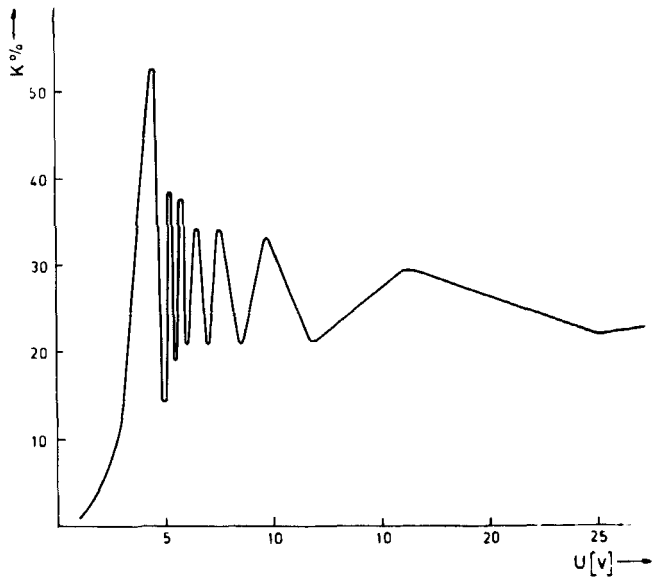

FIGURE 3 Dependence of the steady state intensity of the transmitted light on the voltage. This shape is reconstructed using experimentally determined points of minima and maxima.

K and δ increase gradually with the voltage starting from zero, while in the ideal orientation case no changes of these values could be registered below the threshold voltage.

The light transmitted at zero voltage is (1/30) I_0 which corresponds to $K = 3.3\%$. This signal was compensated in our differential scheme of registration and after this procedure electrooptic effects with K as low as 1% was possible to be registered (see Figure 3 at $V = 1$ V). Further the registration was limited by the noise of the photomultiplier—about 0.2% in units of K (20% of the minimal registered value of K).

On Figure 4 the relaxation behaviour of the system at switching on and off of the electric field applied on the liquid crystal layer is shown for subthreshold voltage. The same for above threshold voltage is shown on Figure 5. Both figures represent the time dependence of the transmitted light intensity on Figure 4, after applying a 3 V rms 7 s pulse and on Figure 5 a 8 V rms 1.5 s pulse. The oscillation after switching off the field on Figure 5 represent the subsequent passing of the intensity of the transmitted light through the four minima which can be seen also on the steady state characteristic—Figure 3 from 0 to 8 V rms. These oscillations are smeared at switching on. They are due to interference of monochromatic light.

The comparison of the two figures shows qualitative difference in the transients following the switching on of the voltage. While for subthreshold

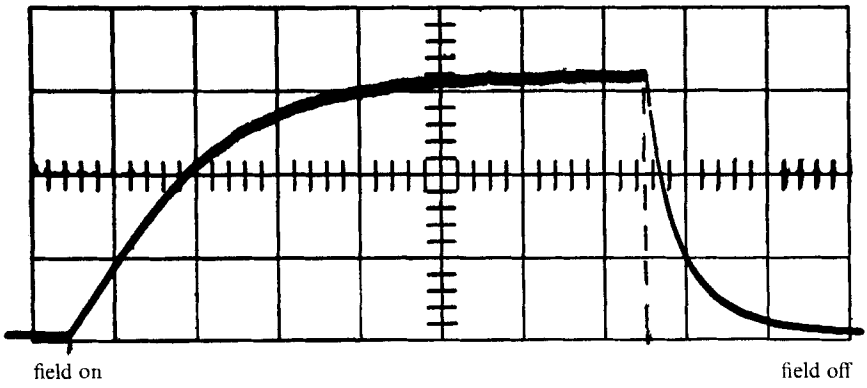

FIGURE 4 Transient behaviour by subthreshold voltages: $V = 3$ V rms, $f = 5$ kHz, sweep 1 s/cm.

voltages the slope of the transient is constantly decreasing, for above threshold voltages it is constantly increasing. This difference provides the possibility not only to determine unambiguously the value of threshold (limiting) voltage but also shows that the threshold character which disappeared in the *steady state* behaviour, in the transient behaviour is clearly manifested. This qualitatively different dynamics was considered in the theoretical part of the paper in details.

The conclusions drawn above are illustrated on Figure 6. On the figure simultaneously the variation with the voltage of the phase differences and rise and decay relaxation times are presented. The relaxation times are

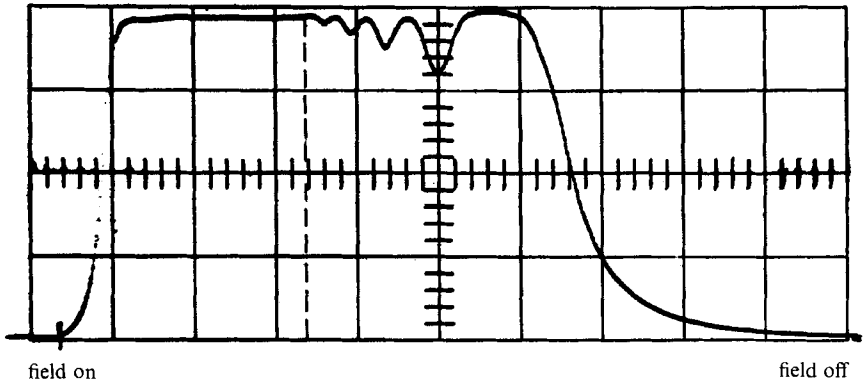

FIGURE 5 Transient behaviour by above threshold voltages: $V = 8$ V rms, $f = 5$ kHz, sweep 0,5 s/cm. The undulations after switching off the field represent the subsequent passing of the intensity of transmitted light through the four minima which can be seen also on the steady-state characteristics—Figure 3, from 0 to 8 V rms. These oscillations are smeared at switching on.

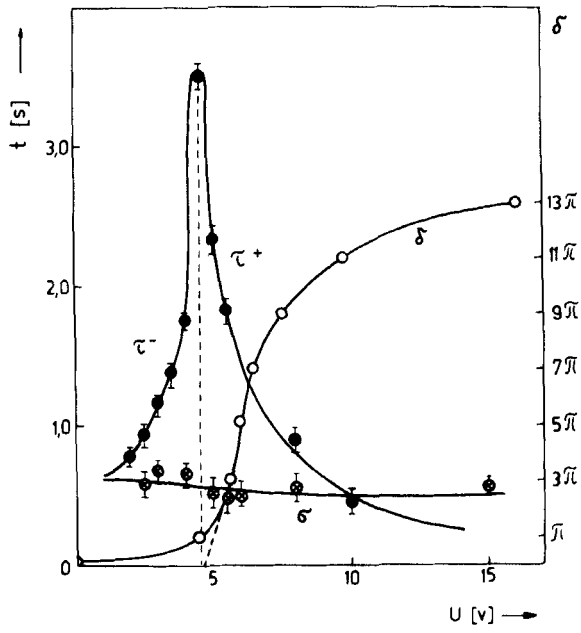

FIGURE 6 Dependence of the relaxation times τ^-, τ^+, σ and phase difference δ on the voltage, $d = 12\ \mu$m.

determined by semilog analysis with the help of theoretical part of the paper. Namely using formula (33) we can write (for small θ)

$$I(t) \sim [\overline{\theta^2(t)}]^2 \sim \theta_M^4(t), \tag{34}$$

where $\overline{\theta^2(t)} = (1/d)\int_{-d/2}^{d/2} \theta^2(z, t)dz$ is the averaged over the whole layer solution. Then taking into account the most slowly relaxating harmonics from the solutions we can write:

Sub threshold regime Switching on: $\theta_M(t)$ from 20′)

$$I(t) = I_\infty - I_{\tau^-} \exp\left(-\frac{t}{\tau^-}\right). \tag{35}$$

Switching off: $\theta_M(t) = \theta_0 + \tilde{\theta}\exp(-t/\sigma^-)$ from (23) or (29)

$$I(t) = I_0 + I_{\sigma^-} \exp\left(-\frac{t}{\sigma^-}\right). \tag{36}$$

Above threshold regime Switching on: θ_M from (20″)

$$I(t) = I_0 \exp\frac{4t}{\tau^+}. \tag{37}$$

Switching off: θ_M like above

$$I(t) = I_0 + I_{\sigma^+} \exp\left(-\frac{t}{\sigma^+}\right). \tag{38}$$

Now having these formulae we are able to calculate from a semilog plot of the transient curve $I(t)$ the corresponding relaxation times. For τ^-, σ^- and σ^+ the tails of the curves are taken (Figure 4 and Figure 5), while for τ^+—the starting points of the curve (Figure 5).

It is seen that at subthreshold voltages the rise times of the effect increase sharply with the increase of the voltage applied. On the contrary at above threshold voltages the rise times decrease with the increase of the voltage. So near the limiting voltage a maximum in the voltage dependence of the transient behaviour exist so that approaching to it from both sides the rise times tend to increase. No similar dependence is observed for the decay times.

4 DISCUSSION AND RESULTS

The experimental and theoretical results obtained on the first place give the possibility to be determined the material constants of the liquid crystal ZLI-207 which participate in the equations and for which there are no other available data in the existing references.

4.1 Determination of the extrapolation length and the constant K_{33}

From the experimental data at different layer thicknesses, the following dependence of the limiting voltage V_c on the layer thickness d is obtained: for $d = 6$, 12 and 27 μm, V_c is respectively 3.5, 4 and 4.5 V.

The critical voltage V_c' is defined as the voltage by which the initial variation of the contrast with the voltage is the steepest. When measuring the $V_c'(d)$ dependence, the same pair of glass plates was used.

According to the equation (14):

$$\frac{1}{V_c'} = \frac{1}{V_c} + \frac{2b}{V_c}\frac{1}{d}$$

i.e. $1/V_c'$ has to be a linear function of $1/d$ with an intercept $1/V_c$ and a slope $2b/V_c$. Fitting the point on Figure 7 with a straight line we determine:

$$V_c = 5\ V;\ b = 1.4\ \mu\text{m}.$$

Knowing the extrapolated value of V_c, from which the influence of the boundary conditions have been already excluded we can determine the

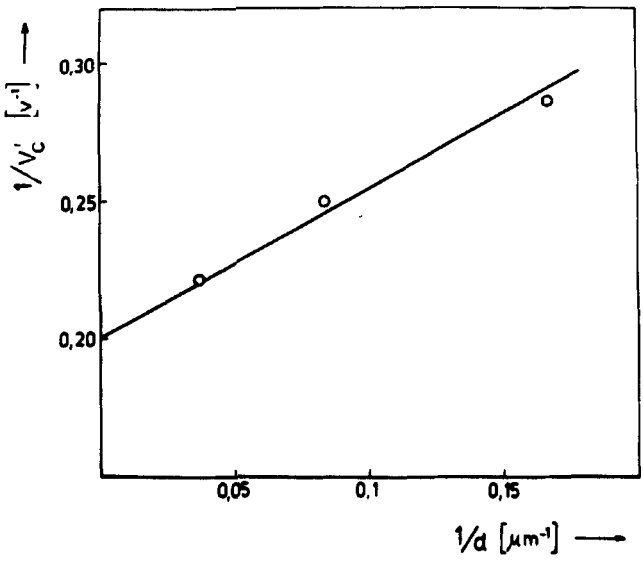

FIGURE 7 Dependence of the reciprocal limiting voltage $1/V_c^1$ on the reciprocal thickness $1/d$.

elastic constant of bending K_{33}. For dielectric anisotropy of ZLI-207 we use the date of Merck.[16]

$$\Delta\varepsilon = -0.6 \qquad \text{i.e. } \Delta\chi = \frac{|\Delta\varepsilon|}{4\pi} = 0.048. \tag{39}$$

Then $K_{33} = 1{,}3 \cdot 10^{-6}$ dyne.

Finally, we determine the anchoring energy

$$C = K_{33}/b = 0{,}9 \cdot 10^{-2} \text{ erg/cm}^2. \tag{40}$$

This value is two order of magnitude greater than the value, obtained by homeotropic orientation, imposed by covering the electrode with lecithin. This result very well corresponds to the data of Gruler[17] according to which when the "orienting" substance is dissolved in the nematic (in his case MBBA) the anchoring energy increases 100 times in comparison with the case of covered electrodes.

4.2 Determination of the viscosity coefficient γ_1^*

From the slope of the dependence of the decay times on the layer thickness using Eq. (32) the following value of the rotational viscosity (including back flow correction) is determined:

$$\gamma_1^* = 3{,}0 \text{ poise} \tag{41}$$

The fit of experimental data with Eq. (24) is worse. Above all it gives an increased value for γ_1^*. It means that in the dynamic behaviour of the system another demonstration of the weak anchoring can be found.

4.3 Relaxation times

The differences in the relaxation behaviour of the system at subthreshold and above threshold regimes in the case of switching on of the electric field were mentioned in the theoretical part of the paper.

As it was seen from the experimental part the times for reaching the steady state sharply increase on both sides of the critical voltage V_c', forming a maximum. The increasing of the rise time with the voltage at subthreshold voltages seems somehow surprising. This calls for the consideration of this question in greater details. The fact that the linear approximation sufficiently well describes the behaviour of the system at subthreshold voltages up to a voltage $V \lesssim (\frac{2}{3})V_c$ shows that in this range the system is stable—the deformations are sufficiently small and the accidental fluctuations are fading. Now let us focus our attention on the relaxation behaviour of the fluctuations. In reference[11] it is shown that in ideally oriented samples all fluctuations at voltage $V < V_c$ are fading exponentially, their time of relaxation coinciding with the relaxation time τ_1^- derived in this paper.

Obviously this relaxation time has to rise with the voltage rising and at $V \to V_c$, τ_d has to tend to the infinity ($\tau_d \to \infty$) which reflects the fact that at the threshold voltage the fluctuations are not fading at all. This critical slowing of the fluctuations together with the divergence of their amplitude results in a pronounced singularity in the scattered light intensity in the ideal orientation case. Similar singularity, although not so strong, was observed in nonideally oriented samples as well (H. Hinov, personal communication).

These considerations give the possibility the following interpretation to be presented of our results. Namely, it could be suggested that the application of a voltage $V < V_c$ displaces the equilibrium state of the system from $\theta_M = \theta_0$ to $\theta_M = \theta_0/\cos((\pi/2)(V/V_c))$ so that it begins to tend to this new state of equilibrium. Then the rise time of the system evidently has to coincide with τ_d, i.e. to increase with the rise of V. The fluctuation behaviour of the system is in concert with this notion and the weak singularity in the scattered light intensity correlates with the maximum in τ vs V dependence.

It is seen on Figure 6 that the times of fading do not depend (essentially) on V. A well followed prediction of the theory concerning the asymptotic behaviour of τ_1 at $V \to 0$:

$$\tau_1 \to \frac{\gamma_1 d_2}{\Delta\chi V_c'^2} = \frac{\gamma_1 d^2}{\alpha_1^2 K_{33}}$$

can be seen on Figure 6 as well.

5 CONCLUSION

It is shown that for liquid crystal layers with a nonideal initial orientation the dynamic characteristics contain qualitatively richer information about the threshold character of the Freedericksz transition in comparison with its steady-state characteristics.

The maximum in the rise time observed permits unambiguous determination of the value of the limiting voltage which is much less clear with the steady-state studies.

The values of some material constants of the liquid crystal mixture ZLI–207 (Merck) are determined as well as the value of the anchoring energy describing the orientational interaction with the substrates.

SUMMARY

The DAP-effect is studied in homeotropic nematic layers of ZLI–207 (Merck) with initial inclination. In such case the effect loses its threshold character and deformations at subthreshold voltages are observed. The dynamics of deformations at switching on and switching off of the voltage is studied theoretically in small angle approximation and experimentally as well. While in the steady state the threshold disappears, threshold character of the effect is preserved in the transient regime. There exist different regimes of deformations with entirely different relaxation turnon behaviour. At subthreshold voltage the relaxation time increases with increasing the voltage. Just the opposite is the behaviour above the threshold. So divergence of the relaxation times is observed at the two sides of the limiting voltage. The observed decrease of the limiting voltage with decreasing of the layer thickness shows that boundary conditions are "soft" and permits us to determine the anchoring energy. The bend elastic constant and the rotational viscosity coefficient for this material are also determined.

References

1. M. F. Schiekel and Fahrenschon, *Appl. Phys. Letters*, **19**, 391 (1971).
2. R. A. Soref and M. J. Rafuse, *J. Appl. Phys.*, **43**, 2029 (1972).
3. F. J. Kahn, *Appl. Phys. Letters*, **20**, 199 (1972).
4. M. Hareng, E. Leiba, and G. Assouline, *Mol. Cryst. Liq. Cryst.*, **17**, 361 (1972).
5. H. Deuling, *Mol. Cryst. Liq. Cryst.*, **19**, 123 (1972).
6. H. Gruler and G. Meier, *Mol. Cryst. Liq. Cryst.*, **16**, 299 (1972).
7. M. Ohtsu, T. Akahane, and T. Tako, *Japan. J. Appl. Phys.*, **13**, 621 (1974).
8. L. Bata, A. Buka, and I. Janossy, *Solid State Comm.*, **15**, 647 (1974).
9. V. Freedericksz and V. Zolina, *Trans. Faraday Soc.*, **29**, 919 (1933).
10. P. Pieranski, F. Brochard, and E. Guyon, *J. Phys.*, **33**, 681 (1972).

11. P. Pieranski, F. Brochard, and E. Guyon, *J. Phys.*, **34**, 35 (1973).
12. F. Brochard-Wyart, These (Universite de Paris-Sud, Orsay A–1271), 1974.
13. A. Rapini and M. Papoular, *J. Phys.* (*suppl.*), **30 C-4**, 54 (1969).
14. F. Broshard, *Mol. Cryst. Liq. Cryst.*, **23**, 51 (1973).
15. E. Guyon, *J. Vac. Sci. Technol.*, **10**, 681 (1973).
16. Nematische Phasen Licristal[R] (Merck 114), 1973, p. 16.
17. H. Gruler, *Z. Naturforsch*, **28a**, 474 (1973).
18. A. Rapini, *J. Phys.*, **34**, 629 (1973).
19. I. Nehring, A. R. Kmetz, and T. J. Scheffer, *J. Appl. Phys.*, **47**, 850 (1976).
20. D. Meyerhofer, *Phys. Letters*, **51A**, 407 (1975).
21. W. Urbach, M. Boix, and E. Guyon, *Appl. Phys. Letters*, **25**, 479 (1974).
22. K. Fahrenschon, H. Gruler, and M. F. Schiekel, *Appl. Phys.*, **11**, 67 (1976).
23. V. Encheva, Diploma Work (Faculty of Physics, University of Sofia), 1974.
24. A. Petrov, S. Sokerov, N. Aneva, and S. Stoylov, *VIIth National Physics Conference, Section Liquid Crystals*, (Vidin, Bulgaria, LOCUS 01353), 1976.
25. S. Sokerov, N. Aneva, P. Stefanov, A. G. Petrov, S. Stoylov, and V. Encheva, *Izv. Khim.*, **9**, 304 (1976).